# Analysis of Compressible Turbulent Flow over a Yawed Cone

A. ROBIN MOWLEM*
*IBM Systems Products Division, East Fishkill Facility, Hopewell Junction, N.Y.*
AND
RUSSELL A. SMITH†
*The Catholic University of America, Washington, D.C.*

## Theme

THE analysis of compressible turbulent flow over a cone at high angle of attack is of current interest in the Space Shuttle program and in the design of high-speed missiles and re-entry vehicles where high maneuverability is an important consideration. This study presents an interesting technique for predicting the appropriate flow parameters. The regime of flow considered is steady-state supersonic to hypersonic flow covering a wide range in angle of attack and including both adiabatic and cold-wall conditions.

## Contents

The analysis assumes ideal gas with a constant Prandtl number of 0.72 and a recovery factor of 0.89. Wall temperature is assumed to be constant throughout. Furthermore the external flow is assumed to be conical, where the fluid properties, like the density and the pressure, do not vary materially along the meridional ray. In addition, the flow is assumed to be steady and wholly turbulent from the apex of the cone. One assumption that is not utilized is the small cross-flow assumption usually found in previous analyses.

Conceptually we have a cone (half-angle $\theta_c$) with the attached shock wrapped around the body surface (Fig. 1). Normally the freestream conditions are known. The pressure distribution may come from an inviscid flow analysis, or from experimental data. Because of the large angles of attack that are considered, cross flow develops necessitating a three-dimensional treatment of the problem. In streamline coordinates this cross flow vanishes at the outer edge of the boundary layer so that great simplifications can be achieved both in the boundary conditions and in the differential equations. Moreover, streamline coordinates provide a convenient system for modeling the physical flow phenomenon, as in the entrainment process, permitting the use of established two-dimensional relationships in the problem solution. This coordinate system as shown in Fig. 1 is based on the projection of the inviscid streamline on the body surface such that the $\xi$ coordinate is along the streamline direction and $\eta$ is the surface coordinate normal to it.

In the usual way the governing equations, i.e., the streamwise momentum equation, the cross-flow equation, and the integrated form of the continuity equation called the entrainment equation, are integrated across the boundary layer. The utility of the method is in the way these governing equations are reduced to simple, easily solved forms. Only the entrainment equation is shown below:

$$\frac{\partial}{\partial s^1}(\theta_{11}H_1)-\frac{\partial\delta_2{}^*}{\partial s^2}=F-\theta_{11}H_1\frac{\partial}{\partial s^1}(\ln\rho_e u_e)-K_1+\delta_2{}^*\left(\frac{\partial}{\partial s^2}(\ln\rho_e u_e)-K_2\right)$$

where $F=F(H_{1K})$.

The velocity defect in the outer layer controls the entrainment of nonturbulent fluid into the layer. This process is expressed in terms of the nondimensional parameter $F$, which is found to be empirically related to the kinematic shape factor $H_{1K}$. Since the equations are in terms of streamline coordinates the cross flow becomes vanishingly small toward the edge of the layer such that the streamwise flow becomes dominant over the cross flow. Therefore one can utilize established two-dimensional relationships, such as two-dimensional velocity profiles.

In essence the governing equations are three coupled, partial, differential equations with ten unknowns—four in momentum thickness, two in displacement thickness, the variable $\beta$ which is the angle of skew of the surface shear stress with respect to the inviscid streamline, a transformed shape factor $\bar{H}$, a streamwise shape factor $H_1$, and the kinematic shape factor $H_{1K}$. The number of unknowns is reduced by five through the use of two-dimensional power-law velocity profiles for both the streamwise and cross-flow profiles, which permit the expression of the thicknesses $\delta_1{}^*$, $\delta_2{}^*$, $\theta_{12}$, $\theta_{21}$, $\theta_{22}$ in terms of the variables $\theta_{11}$, $\bar{H}$, $H_1$, and $\beta$. The system is closed by introducing two empirical correlations, which relate the kinematic shape factor $H_{1K}$ to the streamwise shape factor $H_1$, and the transformed shape factor $\bar{H}$ to $H_1$, i.e., $H_{1K}=H_{1K}(H_1)$ and $\bar{H}=\bar{H}(H_1)$.

Rather than solve the three partial differential equations, they are reduced to ordinary differential equations by assuming the

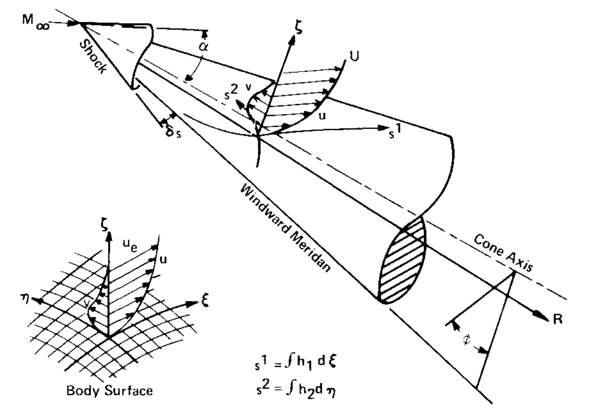


**Fig. 1 Coordinates for boundary-layer flow on cone: $\rho_e$, $u_e$ are density and velocity at the edge of the layer; $K_1$, $K_2$ are geodesic curvature terms; $p$ is static pressure.**

Synoptic received December 27, 1973; revision received April 30, 1974. This Synoptic is based on the Ph.D. dissertation of A. R. Mowlem "Analysis of Compressible Three-Dimensional Turbulent Flow over a Yawed Cone," Catholic University of America, Washington, D.C., 1972, available as Report 73-12467 at the University Microfilms, Xerox Company, 300 North Zeeb Road, Ann Arbor, Mich. 48106 (price available upon request). For details of the analysis presented in the Synoptic and the references cited, the reader is advised to refer to the original dissertation.

Index categories: Boundary Layers and Convective Heat Transfer—Turbulent; Supersonic and Hypersonic Flow; Missile Systems.

* Senior Engineer.

† Associate Professor, Department of Civil and Mechanical Engineering. Member AIAA.

form of the growth of the boundary-layer parameters along $R$. Thus one can set $\theta_{11}$ equal to $f_{11}R^a$ and make it a function of $\phi$ only, and similarly for the other thicknesses; i.e., $\theta_{11} = f_{11}(\phi)R^a$, $\theta_{12} = f_{12}(\phi)R^a$, etc.

For turbulent flow the value of $a$ is determined from the compressible form of the Ludwieg-Tillmann skin-friction law. This value is about 0.8. Because of this assumption the partial derivatives $\partial/\partial s^1$ and $\partial/\partial s^2$ are reduced to ordinary derivatives $d/d\phi$. An additional equation is still required. This is provided by the streamline property equation which relates the direction cosines $l$ and $m$ of the external streamline to the nondimensional circumferential pressure gradient parameter $G$, i.e., $dl/d\phi = lG(\phi) + m \sin\theta_c$. We now have three unknowns—$f_{11}$ instead of $\theta_{11}$, $H_1$, and $\tan\beta$.

Proceeding as before results in a set of working equations which are three ordinary differential equations in three variables, with the $r$, $s$, $t$ coefficients all being nonlinear coefficients which are functions of $\phi$ alone.

### *Working Equations*

Streamwise momentum equation

$$r_1(df_{11}/d\phi) + r_2(dH_1/d\phi) + r_3(d\tan\beta/d\phi) = r_4$$

Cross-flow momentum equation

$$s_1(df_{11}/d\phi) + s_2(dH_1/d\phi) + s_3(d\tan\beta/d\phi) = s_4$$

Entrainment equation

$$t_1(df_{11}/d\phi) + t_2(dH_1/d\phi) + t_3(d\tan\beta/d\phi) = t_4$$

This set of equations is now integrated numerically to obtain the prediction of the flow parameters around the circumference of the cone. However, before the actual integration can begin, initial values of the unknowns $f_{11}$, $H_1$, and $\tan\beta$ are required. These initial values are provided by a solution of the same working equations but applied on the windward meridian. The resulting equations become three highly nonlinear algebraic equations that require an iterative procedure for their solution. This procedure starts with an initial estimate of $H_1$ provided by the incompressible shape factor correlation of Chappell, which is continually refined until a converged value is reached.

The surface heat-transfer distribution is calculated by using a form of the Reynolds analogy equation that relates the Stanton number to the total skin-friction coefficient $C_f$, which is itself

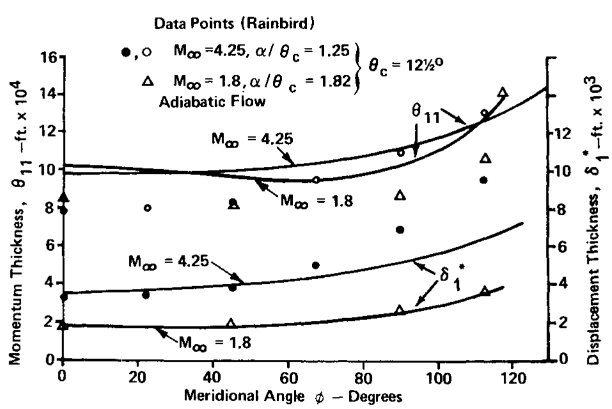


**Fig. 2 Streamwise displacement and momentum thickness distribution.**

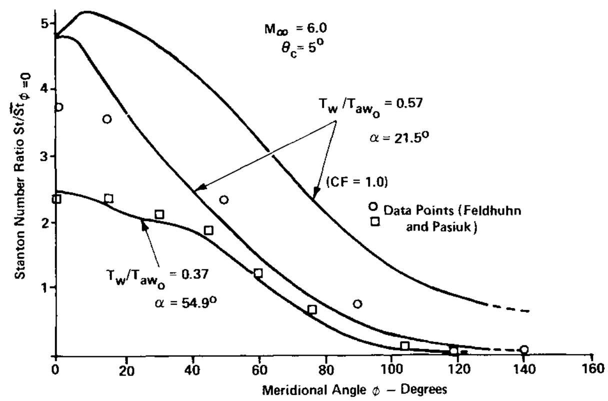


**Fig. 3 Circumferential heat-transfer distribution.**

related to the computed local skin-friction coefficient $C_{f_s}$, i.e., $St = k(C_f/2)$ and $C_f = (C_{f_s}/2)(1+\tan^2\beta)^{1/2}$. The Reynolds analogy factor $k$ depends upon a number of parameters, such as the Prandtl number, and $T_w/T_{aw_o}$, the ratio of wall temperature to the adiabatic wall temperature at the edge of the layer on the windward meridian. For these two factors, the value of $k$ is recommended in the literature to be unity for the conditions of hypersonic flow and cold-wall temperatures. Another factor that $k$ depends on is the circumferential pressure gradient. To account for this effect, a correction factor ($CF$) is derived by utilizing the integral form of the energy equation, and then used to modify the value of the Stanton number ($St$).

With the method of solution that has been described, predictions were made for the flow parameters around the circumference of the cone. These predictions were then compared with experimental data coming from three principal sources: 1) the adiabatic experiments of Rainbird, 2) the heat-transfer experiments of Julius, and 3) the heat-transfer experiments of Feldhuhn and Pasiuk for cold-wall temperatures and high angles of attack. The predictions are compared with experimental data in the set of graphs that follow.

The first graph (Fig. 2) shows the development of the displacement and momentum thicknesses with the angle $\phi$. As can be seen, the agreement between the computed values and the experimental data is excellent for $\delta_1{}^*$, especially up to the angle 80°. For the momentum thickness $\theta_{11}$, the agreement is not quite as good but still quite reasonable. Good comparisons were also achieved in plots (not shown) of the local skin-friction coefficient $C_{f_s}$.

Figure 3 is a plot of the surface heat-transfer distribution. On the vertical axis is shown the ratio of the local Stanton number for turbulent flow normalized by the value of the Stanton number for laminar flow on the windward meridian. One can see that remarkably good agreement has been achieved between experiment and predictions, especially for the very high angle of attack case. The third curve shows that without a correction for circumferential pressure gradient (i.e., with $CF = 1$) predictions would move appreciably away from the data points.

It can be concluded that these results support the method outlined. Moreover, the method can also be extended to nonconical flows for slender bodies, and to regions of adverse pressure gradient.